

# Significant role of the North Icelandic Jet in the formation of Denmark Strait overflow water

Kjetil Våge<sup>1\*</sup>, Robert S. Pickart<sup>2</sup>, Michael A. Spall<sup>2</sup>, Héðinn Valdimarsson<sup>3</sup>, Steingrímur Jónsson<sup>3,4</sup>, Daniel J. Torres<sup>2</sup>, Svein Østerhus<sup>1,5</sup> and Tor Eldevik<sup>1</sup>

**The Denmark Strait overflow water is the largest dense water plume from the Nordic seas to feed the lower limb of the Atlantic Meridional Overturning Circulation. Its primary source is commonly thought to be the East Greenland Current. However, the recent discovery of the North Icelandic Jet—a deep-reaching current that flows along the continental slope of Iceland—has called this view into question. Here we present high-resolution measurements of hydrography and velocity north of Iceland, taken during two shipboard surveys in October 2008 and August 2009. We find that the North Icelandic Jet advects overflow water into the Denmark Strait and constitutes a pathway that is distinct from the East Greenland Current. We estimate that the jet supplies about half of the total overflow transport, and infer that it is the primary source of the densest overflow water. Simulations with an ocean general circulation model suggest that the import of warm, salty water from the North Icelandic Irminger Current and water-mass transformation in the interior Iceland Sea are critical to the formation of the jet. We surmise that the timescale for the renewal of the deepest water in the meridional overturning cell, and its sensitivity to changes in climate, could be different than presently envisaged.**

Oceanographers have been aware of the northern overflows for nearly a century<sup>1</sup>, yet a consensus has still not been reached regarding the origins of the dense water within them. The first definitive scenario for the source of Denmark Strait overflow water (DSOW) implicated open-ocean convection in the central Iceland Sea<sup>2,3</sup> (Fig. 1). Subsequently, it was argued that the transformation of warm Atlantic inflow into DSOW occurs primarily within the cyclonic boundary current system of the Nordic seas, that is with minimal contribution from convection in the central portions of the basins<sup>4</sup>. This notion still prevails today<sup>5</sup>. A central aspect of this scheme is that the East Greenland Current (EGC) is the primary pathway supplying the DSOW (Fig. 1). Compelling new evidence, however, has suggested that a substantial fraction of the Denmark Strait overflow plume is supplied through a previously unidentified current flowing southward along the Iceland continental slope<sup>6</sup>, hereafter called the North Icelandic Jet (NIJ, Fig. 1). This view is supported by sparse mooring data, which show inconsistency between the seasonality of the EGC and the overflow water<sup>7,8</sup>.

## Water masses of the Denmark Strait overflow

In general, water denser than  $\sigma_\theta = 27.8 \text{ kg m}^{-3}$  is identified as overflow water<sup>9</sup>. We adopt this definition as well, and require furthermore that, upstream of the strait, the overflow water be situated above sill depth (here taken to be 650 m). Transports calculated for the full water column give similar results. Defined as such, overflow water resides in the intermediate layer of the Nordic seas. To avoid complex nomenclature, which is unnecessary in the context of the present study, we distinguish only two types of intermediate water: Atlantic-origin water and Arctic-origin water, warmer and colder than  $0^\circ\text{C}$ , respectively<sup>10,11</sup>. Although the Atlantic Ocean is ultimately the source of most of the water in the Nordic seas, these two labels refer to the geographical domain in which the transformation from surface to intermediate water masses takes place<sup>3</sup>. In

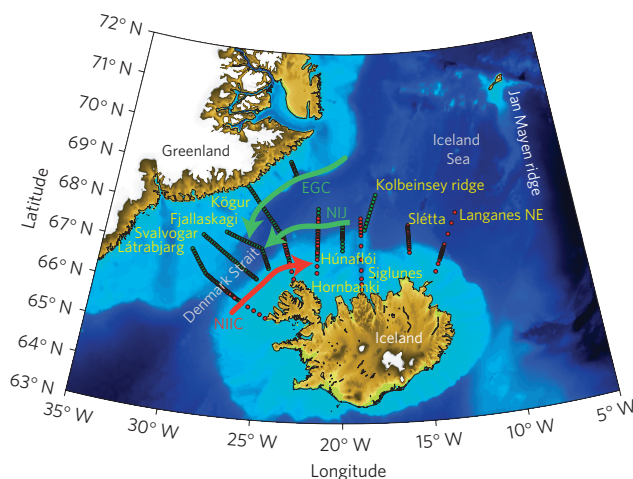


**Figure 1 | Flow through the Denmark Strait.** Stations from the October 2008 and August 2009 surveys are marked in green and red, respectively. The sections are referred to by names (the names originate from nearby features along the Icelandic coast). EGC, East Greenland Current; NIJ, North Icelandic Jet; NIIC, North Icelandic Irminger Current.

particular, Atlantic-origin water is densified primarily within the northward-flowing boundary current along the Norwegian continental slope, whereas Arctic-origin water results from wintertime convection within the interior Greenland and Iceland seas.

The October 2008 occupation of the Látrabjarg line, a short distance downstream of the Denmark Strait sill, provides an illustration of these two broad classes of intermediate water (Fig. 2). The deepest part of the strait was filled by a bolus of uniform, dense water (Fig. 2a–c)—a configuration commonly observed in

<sup>1</sup>Geophysical Institute and Bjerknes Centre for Climate Research, University of Bergen, 5007 Bergen, Norway, <sup>2</sup>Woods Hole Oceanographic Institution, Woods Hole, Massachusetts 02543, USA, <sup>3</sup>Marine Research Institute, 101 Reykjavik, Iceland, <sup>4</sup>University of Akureyri, 600 Akureyri, Iceland, <sup>5</sup>Uni Bjerknes Centre, Uni Research, 5007 Bergen, Norway. \*e-mail: kjetil.vage@gfi.uib.no.

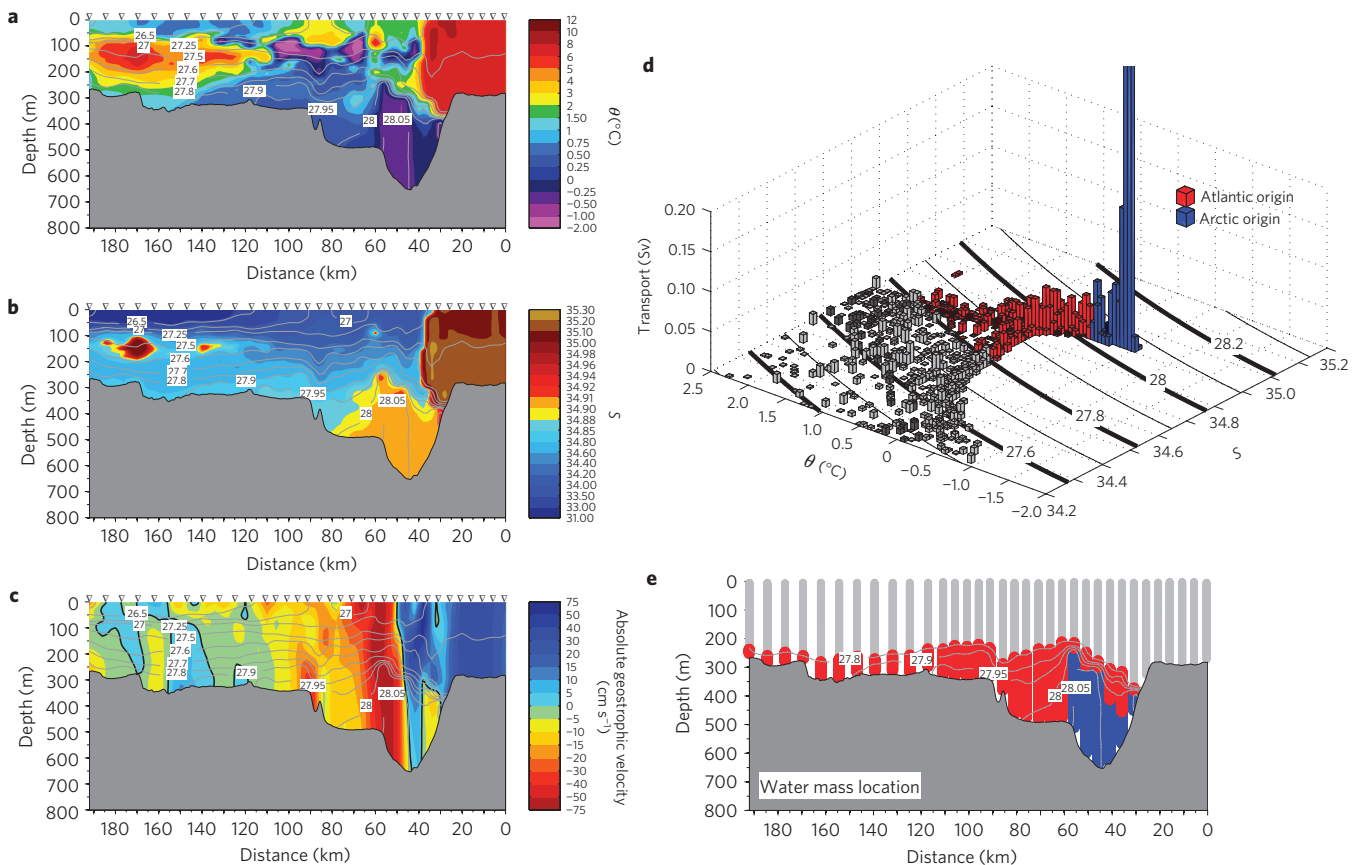


**Figure 2 | Hydrographic properties along the Látrabjarg line near the sill as measured during the October 2008 survey. a–c,** Vertical sections (in colour) of potential temperature ( $^{\circ}\text{C}$ ), salinity and absolutely referenced geostrophic velocity ( $\text{cm s}^{-1}$ , equatorward flow is negative), respectively. **d,** Transport  $\theta$ – $S$  diagram (the few columns representing a net northward flow of overflow water are darkened). **e,** Geographic location of the water masses highlighted in **d**. The grey lines in **a–c** and **e** are contours of potential density ( $\text{kg m}^{-3}$ ), and the black lines in **c** are the zero-velocity contour. The triangles indicate station locations.

the Denmark Strait linked to the formation of cyclonic vortices<sup>12</sup>. When partitioning the transport of the overflow layer in potential temperature ( $\theta$ )–salinity ( $S$ ) space (Fig. 2d), we found that a large portion of the Arctic-origin component is contained within the bolus (the narrow, sharp peak of very dense water), whereas the Atlantic-origin water is distributed over a wider hydrographic range. The total volume fluxes of the components were comparable,  $1.9 \pm 0.6 \text{ Sv}$  versus  $1.8 \pm 0.3 \text{ Sv}$  for Atlantic- and Arctic-origin waters, respectively ( $1 \text{ Sv} = 10^6 \text{ m}^3 \text{ s}^{-1}$ ). However, the denser Arctic-origin water occupied the deepest part of the strait, whereas the Atlantic-origin water was primarily found on the Greenland shelf (Fig. 2e). It is believed that a significant fraction of the latter water mass remains on the Greenland shelf and consequently does not contribute to the DSOW plume<sup>13,14</sup>. Hence, the dense Arctic-origin water may represent a large fraction of the traditional plume observed in the deep Irminger Sea.

### Pathway and transport of the NIJ

Recently, the NIJ was invoked as a potential source of DSOW on the basis of direct shipboard velocity measurements collected northwest of Iceland<sup>6</sup>. The current was observed to be largely barotropic and potentially of sufficient strength to account for the known transport of DSOW across the sill if some entrainment of ambient water was included. We note that these observations were limited geographically (primarily obtained at one location), and that there was little or no concurrent hydrography.

The sections north of the sill in Fig. 1 reveal that Atlantic-origin water resided primarily on the Greenland slope, with a portion

spreading into the interior, whereas Arctic-origin water was found solely on the Iceland slope (not shown). The densest overflow water ( $\sigma_{\theta} \geq 28.03 \text{ kg m}^{-3}$ ) resided on the Iceland slope at each of the hydrographic sections (Fig. 3, colour). This up-tilt of deep isopycnals onto the Iceland slope has been noted in previous studies<sup>6</sup>, but was typically thought to reflect the recirculation of dense EGC water to the northeast. Such an interpretation was based on unreferenced thermal wind shear, which implies a bottom-intensified northward current of water too dense to cross the sill<sup>10</sup>. Our absolutely referenced geostrophic velocities indicate instead that this dense water flows southward towards the Denmark Strait (Fig. 3, vectors).

The vertical sections of velocity and density across the Iceland slope reveal a consistent hydrographic and dynamical structure of the NIJ at all locations (see Supplementary Information), with some section-to-section variability probably due to mesoscale processes. The jet is narrow (often less than 20 km wide, in agreement with previous measurements<sup>6</sup>) and is centred near the 650 m isobath, which is also the depth of the Denmark Strait sill. The NIJ is weakly baroclinic, with a mid-depth maximum. Both surveys show that the current is present to the east of the Kolbeinsey ridge (the continuation of the Mid-Atlantic Ridge north of Iceland) and hence it is an independent pathway distinct from the EGC. We note, however, that closer to the Denmark Strait there could be a contribution from the EGC, as suggested by recent high-resolution model simulations<sup>15</sup>.

It is well known that the transport of DSOW at the Denmark Strait sill varies significantly on short timescales of a few days<sup>16–18</sup>; this is decoupled from the longer-period variations of the flow

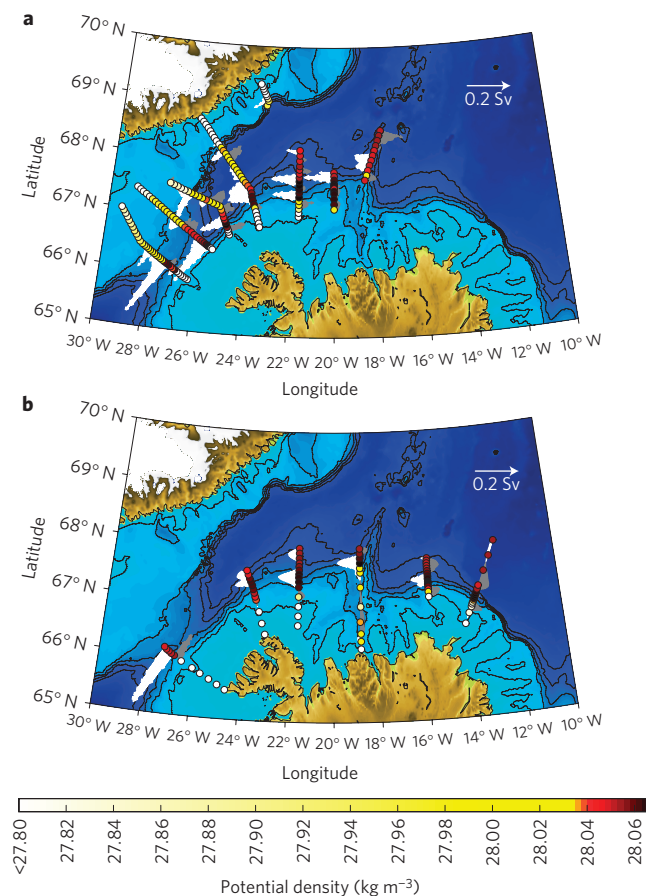


**Figure 3 | Flow of dense water upstream of the Denmark Strait. a, b,** The colours indicate the maximum potential density at each station and the white and grey vectors show the magnitude of the transport (in Sv) per 2 km segment towards and away from the Denmark Strait, respectively, from October 2008 (**a**) and August 2009 (**b**). Only the portion of the water column that can directly participate in the overflow ( $\sigma_{\theta} \geq 27.8 \text{ kg m}^{-3}$  and depth  $< 650 \text{ m}$ ) is considered in the figure. The 200 m, 400 m, 600 m, 800 m and 1,000 m isobaths are contoured.

upstream<sup>7,16</sup>. Therefore, to obtain a more robust estimate of the transport at the sill with which to compare our upstream measurements, we considered other synoptic velocity crossings near the Látrabjarg line<sup>9</sup> (see the Methods section for details on the origin of the extra sections). Using a total of nine sections (including ours), the mean transport of overflow water ( $\sigma_{\theta} \geq 27.8 \text{ kg m}^{-3}$ ) is  $2.9 \pm 0.5 \text{ Sv}$ . For the densest component ( $\sigma_{\theta} \geq 28.03 \text{ kg m}^{-3}$ ), the value is  $0.6 \pm 0.2 \text{ Sv}$ . The corresponding estimates for the NIJ upstream of the sill from our two surveys are  $1.5 \pm 0.2 \text{ Sv}$  and  $0.6 \pm 0.1 \text{ Sv}$ , respectively. This implies that the NIJ can account for roughly half of the total overflow transport, and nearly all of the densest component. This is consistent as well with mooring-based estimates of 2.9–3.7 Sv (refs 17,18) (these refer to the total overflow transport only). If we relax our constraint of 650 m and consider all of the dense water advected by the NIJ (including the portion below sill depth), less than 0.1 Sv is added. This suggests that the process of aspiration, believed to be at work in the Strait of Gibraltar and in the Faroe Bank Channel<sup>19–21</sup>, does not play an important role at the Denmark Strait (though some contribution from aspiration cannot be discounted).

### Formation of the NIJ

To help identify the source of the cold, dense outflowing NIJ, an idealized configuration of the MITgcm primitive equation oceanic

general circulation model<sup>22</sup> was run. It is not our intention to produce a comprehensive simulation of the circulation in the northern North Atlantic and Nordic seas. Instead, we aim to construct a simplified model of the region that includes the key elements required to produce analogues of the main observed currents and water-mass transformations—namely, (1) a sill that separates a subpolar gyre from a marginal sea; (2) an island located along the sill; (3) buoyancy loss in the marginal sea and (4) cyclonic wind stress curl (see the Methods section and ref. 23 for details of the model). Despite its simplicity, the model reproduces many of the essential elements of the circulation and hydrography of the northern subpolar gyre and southern Nordic seas (Fig. 4). This suggests that, although further complexities such as topographic ridges, the Arctic Ocean and haline forcing may also play a role, they are not essential to the basic current structure of interest here.

The densest water in the model is found in the interior of the marginal sea, where convection occurs and the mean flow is weak. There are three inflowing branches of warm water into the marginal sea: along the eastern boundary, east of the island and along the western boundary of the island. The latter is the model equivalent of the NIIC. Note that the warm signal of the model NIIC erodes as it progresses around the island, becoming more dense (Fig. 4a,b). Hydrographic and drifter data suggest that there is a similar densification and disintegration of the observed NIIC as it flows along the north slope of Iceland<sup>24,25</sup>. This begs the question of what happens to the inflowing transport of the NIIC.

The model has two distinct dense, southward-flowing currents to the west of the island and one dense overflow to the east of the island (the latter is the model equivalent of the Faroe Bank Channel overflow). The largest southward transport (approximately 8 Sv) occurs in the current adjacent to the western boundary, similar to the observed EGC transport<sup>26</sup>. Note, however, that much of the water in this current is lighter than the water formed by convection in the basin interior. The second southward-flowing current west of the island resides below the warm, inflowing NIIC and transports the densest water towards the sill. This current is formed primarily along the coast of the island (Fig. 4b) and is the model equivalent of the NIJ. Its transport increases as it flows southward and reaches 1.4 Sv at the sill, similar to the observed NIJ (Fig. 4b–c).

Nearly two-thirds of this transport originates from vertical advection along the coast of the island, about one-third is due to lateral entrainment from the cyclonic interior recirculation gyre and a small portion comes from east of the island. Lateral entrainment into the NIJ has been discussed in previous general circulation models<sup>15</sup>, so we focus here on the first process, which involves densification and downwelling north of the island, and demonstrates a dynamical link between the inflowing NIIC and outflowing NIJ.

Consider first the densification, that is, the water-mass transformation. As the warm NIIC progresses around the island it is cooled by the atmosphere directly above, and consequently the mixed layer within the current deepens. However, the mixed-layer depth remains relatively shallow ( $< 250 \text{ m}$ ). By contrast, the atmospheric cooling in the weakly stratified basin interior, north and west of the island, drives deep convection, forming a denser water mass. This heat loss in the interior is balanced by a lateral flux of water from the baroclinically unstable NIIC. Note that the lateral exchange with the basin interior densifies the NIIC to a greater degree than the local cooling within the current from above.

Now consider the regional sinking that feeds the NIJ. Most of the vertical transport is due to downwelling within the upper 400 m, as indicated by the profile of the vertical transport integrated over the region of the NIJ (Fig. 4d). There is also a smaller contribution due to upwelling from below the sill depth, which is carried primarily in the bottom boundary layer below the NIJ. Despite the strong water-mass conversion in the interior convection



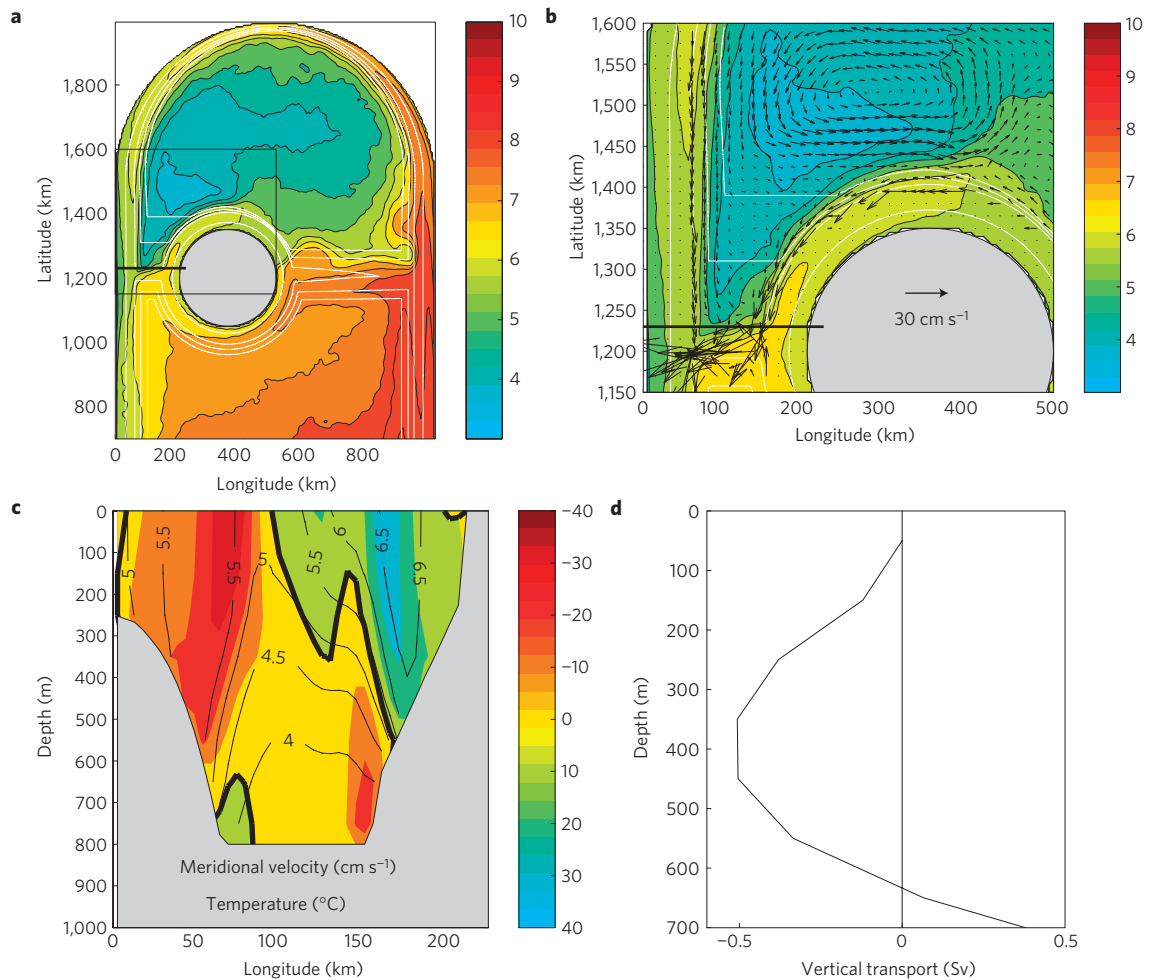


**Figure 4 | Model circulation and hydrography.** **a**, Mean sea surface temperature in the northern model domain (colours; contour interval, 0.5 °C) and bottom topography (white contours; contour interval, 400 m). **b**, Mean sea surface temperature, bottom topography and horizontal velocity at 650 m depth (every third vector) within the box indicated in **a**. **c**, Vertical sections of mean meridional velocity (colour; negative equatorward; contour interval, 5 cm s<sup>-1</sup>; zero line bold) and temperature (black contours; contour interval, 0.5 °C) at the bold line in **a**. **d**, Profile of vertical transport integrated over the region north of the sill, south of 1,550 km latitude and between 125 km and 550 km longitude.

region, the net downwelling there (that is the vertical mass transport) is negligible<sup>27,28</sup>. Instead, the sinking occurs adjacent to the continental boundary of the island. This is understood by realizing that a re-organization of mass is required to maintain the thermal wind balance in the boundary current system. In particular, the lateral density difference between the boundary and the interior decreases as we progress northward and eastward around the island (the NIIC becomes more dense, whereas the water in the interior remains essentially uniform). For the along-boundary flow to maintain thermal wind balance, the vertical shear in the along-boundary velocity must decrease as the density on the boundary increases. This is achieved by a net downwelling of mass within the boundary current<sup>28</sup>, which feeds the NIJ. We emphasize that the densification (transformation) occurs primarily offshore in the basin interior, whereas the sinking (net vertical mass flux) of the dense water occurs near the boundary; they are distinct processes that are linked through the lateral eddy heat flux.

The observations and the model both indicate that a significant fraction of the total DSOW—and the majority of the densest component—is supplied by the NIJ. The current originates along the northern coast of Iceland, which contradicts the notion accepted at present that the DSOW stems primarily from the EGC. Our results implicate water-mass transformation in the central Iceland Sea and the NIIC/NIJ current system as central components to the

deep limb of the Atlantic Meridional Overturning Circulation, and raise new questions as to how the overturning cell will respond to future changes in climate.

## Methods

The two high-resolution hydrographic/velocity surveys considered here were carried out in October 2008 on the R/V *Knorr* (KN194) and in August 2009 on the R/V *Bjarni Sæmundsson* (BS10-2009). The hydrographic measurements were obtained using a Sea-Bird conductivity–temperature–depth instrument. On the basis of laboratory calibrations, the accuracies of the temperature and pressure measurements are 0.001 °C and 0.3 dbar, respectively. On the basis of *in situ* calibration of the conductivity sensor (using deep-water sample data), the accuracy of the salinity measurement is 0.002. Velocities were measured using acoustic Doppler current profiler (ADCP) instruments: a vessel-mounted ADCP on the October 2008 survey and an upward- and downward-facing lowered ADCP system on the August 2009 survey. An updated version of the Oregon State University Atlantic Ocean tidal model<sup>29,30</sup> was used to remove the barotropic tidal component from the ADCP velocities. Gridded 2 km by 10 m fields of potential temperature, salinity, potential density and velocity for each section were constructed using Laplacian-spline interpolation. Using the temperature and salinity fields, the relative geostrophic flow normal to each section was calculated, which was then referenced by matching the vertically averaged relative and ADCP velocities (between 50 and 500 m) at each horizontal grid point<sup>13</sup>.

ADCP instrument error and inaccurate bathymetry in the tidal model were the primary sources of uncertainty associated with the absolutely referenced geostrophic velocities, whereas flow through the 'bottom triangles', that is the area below the deepest common level of neighbouring hydrographic stations, resulted in a negligible error because of the short distance between stations. The standard



deviation of on-station measurements, which were made in close proximity both spatially and temporally, was used to assess the uncertainty of the shipboard ADCP instrument. Comparison between down- and up-cast measurements as well as formal errors calculated during the data-processing stage<sup>31</sup> were used to assess the uncertainty of the lowered ADCP instrument system. In both cases the instrument error was estimated to be approximately  $\pm 3 \text{ cm s}^{-1}$ . Differences between observed and model depths scaled by the magnitude of the tidal flow resulted in a tidal-model error estimate of  $\pm 2 \text{ cm s}^{-1}$ . The total uncertainty was determined as the root of the sum of the squares of the instrument and tidal-model errors. For the transport calculations it was not assumed that the error was uncorrelated across the array, which resulted in a conservative estimate of transport errors. The transport error estimates for three sections were further enlarged by  $0.3 \text{ Sv}$  in a root sum square sense, approximately corresponding to an uncertainty of  $5 \text{ km}$  in the lateral extent of a  $10 \text{ cm s}^{-1}$  barotropic flow over  $650 \text{ m}$  depth. The sections in question are the two realizations of the Kögur line, where a confluence between the NIJ and an offshore flow took place, and the October 2008 Húnaflói section, which is possibly underestimated owing to limited offshore sampling (though the core of the NIJ was sufficiently bracketed, see Supplementary Information). To obtain a more robust estimate of the transport near the Látrabjarg line we used seven further sections of absolutely referenced geostrophic velocity from a survey carried out in September 1998 on the R/V *Poseidon*<sup>9</sup>.

The model domain is  $2,000 \text{ km}$  in the meridional direction and  $1,000 \text{ km}$  in the zonal direction with a maximum depth of  $2,000 \text{ m}$ . A  $650\text{-m}$ -deep sill is located at  $1,200 \text{ km}$  latitude, which separates the domain into a southern subpolar gyre and a northern marginal sea (the Nordic seas). An island  $300 \text{ km}$  in diameter representing Iceland is located at the sill latitude and  $350 \text{ km}$  from the western boundary. The model is forced at the surface with a zonal wind stress  $\tau = \tau_0 \cos(\pi y/L)$ , where  $L$  is the meridional extent of the basin,  $y$  is the meridional coordinate and  $\tau_0 = 0.15 \text{ N m}^{-2}$ . The upper layer temperature is restored towards an atmospheric temperature that decreases from  $10^\circ \text{C}$  at  $y = 0$  to  $2^\circ \text{C}$  in the northwest corner of the basin with a timescale of 60 days. The stratification south of  $y = 200 \text{ km}$  is relaxed towards a uniform stratification of  $N^2 = -g/\rho_0 \partial \rho / \partial z = 2 \times 10^{-6} \text{ s}^{-2}$ , where  $\rho$  is the density,  $\rho_0$  is a reference density and  $z$  is the vertical coordinate. The horizontal grid spacing is  $5 \text{ km}$  and there are 20 uniformly spaced levels in the vertical. The model was started at rest and run for a period of 30 years. The results shown in Fig. 4 are mean values calculated over the final 5 years of integration. Further details can be found in ref. 23, which uses a similar configuration without an island.

Received 26 January 2011; accepted 15 July 2011; published online 21 August 2011

## References

- Nansen, F. Das Bodenwasser und die Abkühlung des Meeres. *Int. Rev. Gesamten Hydrobiol. Hydrogr.* **5**, 1–42 (1912).
- Swift, J. H., Aagaard, K. & Malmberg, S.-A. The contribution of the Denmark Strait overflow to the deep North Atlantic. *Deep-Sea Res.* **27A**, 29–42 (1980).
- Swift, J. H. & Aagaard, K. Seasonal transitions and water mass formation in the Iceland and Greenland seas. *Deep-Sea Res.* **28A**, 1107–1129 (1981).
- Mauritzen, C. Production of dense overflow waters feeding the North Atlantic across the Greenland–Scotland Ridge. Part 1: Evidence for a revised circulation scheme. *Deep-Sea Res.* **1** **43**, 769–806 (1996).
- Eldevik, T. *et al.* Observed sources and variability of Nordic seas overflow. *Nature Geosci.* **2**, 406–410 (2009).
- Jónsson, S. & Valdimarsson, H. A new path for the Denmark Strait overflow water from the Iceland Sea to Denmark Strait. *Geophys. Res. Lett.* **31**, L03305 (2004).
- Jónsson, S. *The Circulation in the Northern Part of the Denmark Strait and its Variability*. ICES Report CM-1999/L:06 (ICES, 1999).
- Dickson, R. R. & Brown, J. The production of North Atlantic deep water: Sources, rates and pathways. *J. Geophys. Res.* **99**, 12319–12341 (1994).
- Girton, J. B., Sanford, T. B. & Käse, R. H. Synoptic sections of the Denmark Strait overflow. *Geophys. Res. Lett.* **28**, 1619–1622 (2001).
- Rudels, B., Fahrbach, E., Meincke, J., Budéus, G. & Eriksson, P. The East Greenland Current and its contribution to the Denmark Strait overflow. *ICES J. Mar. Sci.* **59**, 1133–1154 (2002).
- Rudels, B. *et al.* The interaction between waters from the Arctic Ocean and the Nordic Seas north of Fram Strait and along the East Greenland Current: Results from the Arctic Ocean-02 Oden expedition. *J. Mar. Syst.* **55**, 1–30 (2005).
- Spall, M. A. & Price, J. F. Mesoscale variability in Denmark Strait: The PV outflow hypothesis. *J. Phys. Oceanogr.* **28**, 1598–1623 (1998).
- Pickart, R. S., Torres, D. J. & Fratantoni, P. S. The East Greenland Spill Jet. *J. Phys. Oceanogr.* **35**, 1037–1053 (2005).
- Magaldi, M. G., Haine, T. W. N. & Pickart, R. S. On the nature and variability of the East Greenland Spill Jet: A case study in summer 2003. *J. Phys. Oceanogr.* <http://dx.doi.org/10.1175/JPO-D-10-05004.1> (in the press).
- Köhl, A., Käse, R. H. & Stammer, D. B. Causes of changes in the Denmark Strait overflow. *J. Phys. Oceanogr.* **37**, 1678–1696 (2007).
- Smith, P. C. Baroclinic instability in the Denmark Strait overflow. *J. Phys. Oceanogr.* **6**, 355–371 (1976).
- Ross, C. K. Temperature–salinity characteristics of the ‘overflow’ water in Denmark Strait during ‘OVERFLOW ’73’. *Rapp. P.-v. Réun.-Cons. Int. Explor. Mer.* **185**, 111–119 (1984).
- Macrander, A., Send, U., Valdimarsson, H., Jónsson, S. & Käse, R. H. Interannual changes in the overflow from the Nordic Seas into the Atlantic Ocean through Denmark Strait. *Geophys. Res. Lett.* **32**, L06606 (2005).
- Stommel, H., Bryden, H. & Mangelsdorf, P. Does some of the Mediterranean outflow come from great depth? *Pure Appl. Geophys.* **105**, 879–889 (1973).
- Kinder, T. H. & Parrilla, G. Yes, some of the Mediterranean outflow does come from great depth. *J. Geophys. Res.* **92**, 2901–2906 (1987).
- Hansen, B. & Østerhus, S. Faroe Bank Channel overflow 1995–2001. *Prog. Oceanogr.* **75**, 817–856 (2007).
- Marshall, J., Hill, C., Perelman, L. & Adcroft, A. Hydrostatic, quasi-hydrostatic, and nonhydrostatic ocean modeling. *J. Geophys. Res.* **102**, 5733–5752 (1997).
- Spall, M. A. On the role of eddies and surface forcing in the heat transport and overturning circulation in marginal seas. *J. Clim.* <http://dx.doi.org/10.1175/2011JCLI4130.1> (2011).
- Stefánsson, U. North Icelandic waters. *Rit Fiskid.* **3**, 1–269 (1962).
- Valdimarsson, H. & Malmberg, S.-A. Near-surface circulation in Icelandic waters derived from satellite tracked drifters. *Rit Fiskid.* **16**, 23–39 (1999).
- Woodgate, R. A., Fahrbach, E. & Rohardt, G. Structure and transports of the East Greenland Current at  $75^\circ \text{N}$  from moored current meters. *J. Geophys. Res.* **104**, 18059–18072 (1999).
- Spall, M. A. Boundary currents and watermass transformation in marginal seas. *J. Phys. Oceanogr.* **34**, 1197–1213 (2004).
- Spall, M. A. Dynamics of downwelling in an eddy-resolving convective basin. *J. Phys. Oceanogr.* **40**, 2341–2347 (2010).
- Egbert, G. D., Bennett, A. F. & Foreman, M. G. G. TOPEX/Poseidon tides estimated using a global inverse model. *J. Geophys. Res.* **99**, 24821–24852 (1994).
- Egbert, G. D. & Erofeeva, S. Y. Efficient inverse modeling of barotropic ocean tides. *J. Atmos. Oceanic Technol.* **19**, 183–204 (2002).
- Thurnherr, A. M. A practical assessment of the errors associated with full-depth LADCP profiles obtained using Teledyne RDI Workhorse Acoustic Current Doppler Profilers. *J. Atmos. Oceanic Technol.* **27**, 1215–1227 (2010).

## Acknowledgements

The authors wish to thank B. Rudels and J. B. Girton for comments. Support for this work was provided by the US National Science Foundation and the Research Council of Norway. This is publication A351 from the Bjerknes Centre for Climate Research.

## Author contributions

K.V., R.S.P., H.V., S.J. and D.J.T. collected and analysed the data; M.A.S. designed and analysed the model simulations; K.V., R.S.P. and M.A.S. wrote the paper and all authors interpreted the results and clarified the implications.

## Additional information

The authors declare no competing financial interests. Supplementary information accompanies this paper on [www.nature.com/naturegeoscience](http://www.nature.com/naturegeoscience). Reprints and permissions information is available online at <http://www.nature.com/reprints>. Correspondence and requests for materials should be addressed to K.V.